HEAT FLUX AND WALL TEMPERATURE ESTIMATES FOR THE NASA LANGLEY HIFiRE DIRECT CONNECT RIG

Vincent Cuda, Jr.
ATK Space Division
Hampton, Virginia 23681

&

Neal E. Hass
NASA Langley Research Center
Hampton, Virginia 23681

ABSTRACT

An objective of the **H**ypersonic **I**nternational **Fl**ight **R**esearch **E**xperimentation (HIFiRE) Program Flight 2 is to provide validation data for high enthalpy scramjet prediction tools through a single flight test and accompanying ground tests of the HIFiRE Direct Connect Rig (HDCR) tested in the NASA LaRC Arc Heated Scramjet Test Facility (AHSTF). The HDCR is a full-scale, copper heat sink structure designed to simulate the isolator entrance conditions and isolator, pilot, and combustor section of the HIFiRE flight test experiment flowpath and is fully instrumented to assess combustion performance over a range of operating conditions simulating flight from Mach 5.5 to 8.5 and for various fueling schemes. As part of the instrumentation package, temperature and heat flux sensors were provided along the flowpath surface and also imbedded in the structure. The purpose of this paper is to demonstrate that the surface heat flux and wall temperature of the Zirconia coated copper wall can be obtained with a water-cooled heat flux gage and a sub-surface temperature measurement. An algorithm was developed which used these two measurements to reconstruct the surface conditions along the flowpath. Determinations of the surface conditions of the Zirconia coating were conducted for a variety of conditions.

INTRODUCTION

The HIFiRE Program is a bi-lateral collaboration executed by an integrated team representing the U.S. Air Force Research Laboratory (AFRL) and the Australian Defence Science and Technology Organization (DSTO). Further, the US Air Force has secured a Space Act Agreement with NASA to advance the collaborative development and demonstration of hypersonic aero-propulsion technologies. The objective of the HIFiRE Program is to increase understanding of fundamental hypersonic phenomena and to develop technologies deemed critical to the realization of next generation aerospace vehicles. The purpose is to extend the hypersonic database and enhance the accuracy of complex models and simulations. Phenomena will be examined and characterized at flight conditions that are difficult, if not impossible, to model with current computational methods and/or simulate in ground test facilities. The product of this program is an experimental flight laboratory to capture extensive coherent high-fidelity data. The scope of this program encompasses a series of 8 focused research projects.

The demonstration of sustainable scramjet combustion for an airbreathing engine will enable designers to build aircraft that can fly in the hypersonic regime. Ground tests for both hydrogen and hydrocarbon-fueled scramjet combustors have proven the viability of this technology (reference 1). The successful Hyper-X Program demonstrated that hydrogen combustion for a free flying airframe was sustainable for the specific design points at Mach 7 and Mach 10, at a dynamic pressure (DP) of 1000 lbf/ft^2 (reference 2). Current efforts focus on demonstrating hydrocarbon combustion under similar flight conditions but over a continuous range of Mach numbers. To meet these research objectives, the HIFiRE Program will attach a scramjet flowpath to a Pedro Oriole sounding rocket to provide Mach 5.5 to 8.5 conditions for the engine test (reference 3). In order to mitigate risk, the HIFiRE Program initiated a series of ground tests to verify the operability of the flight engine flowpath and injector design to ensure that both ramjet and scramjet combustion could be obtained for a range of fueling schedules. Ground tests were performed in the NASA Langley AHSTF which served as the test bed for the engine design (reference 1).

An objective of the HIFiRE ground tests was the mapping of the thermal response of the model to a variety of test conditions and fueling schedules. One area of interest was in estimating the heating to the HDCR that resulted from the combustion process. The HDCR flowpath was constructed with 2 inch thick copper walls that were thermally protected with a thin zirconium dioxide (commonly referred to as Zirconia) coating. Both heat flux transducers and thermocouples were installed in various configurations along the flowpath. It was known that just by placing a heat flux transducer flush with the flowpath wall would provide measurements that were inconsistent with the expected heat flux at the Zirconia surface. This was due to the vastly different temperatures of the sensor and the Zirconia wall. Since the HDCR was designed with an instrumentation suite that included heat flux and temperature measurements, a method to determine the surface conditions at the Zirconia wall was sought.

THE LANGLEY ARC-HEATED SCRAMJET TEST FACILITY AND HIFIRE DIRECT CONNECT RIG

The AHSTF is used for tests of component models of airframe integrated scramjet engines at conditions experienced at flight Mach numbers between 4.7 to 8 (references 4 and 5). The arc-heater and test section of the AHSTF facility are located in room 111 of building 1247B at Langley Research Center in Hampton, Virginia. Test results are used to assess the performance of scramjet engines, to optimize the design of the components, and to optimize fueling schemes. Historically, models have included an inlet, isolator, combustor, and a significant portion of the nozzle. For the HIFiRE Program, tests were performed in a direct connect mode for the first time, where the facility nozzle produced flow to simulate the inlet exit/isolator entrance conditions.

To verify both the performance and operability of the HIFiRE engine, the HDCR was developed to model a full scale version of the flight isolator, combustor, and the fuel injectors (reference 6). The HDCR was installed in the AHSTF (see Figure 1) to reproduce the test conditions of interest. The model was constructed of Oxygen Free High Conductivity (OFHC) copper and was instrumented with pressure taps, thermocouples, and heat flux transducers. The HIFiRE Engine Assembly was 28” x 10” x 7.9” and weighed 418 lbm. The walls were 2” thick to ensure that engine tests would have a sufficient runtime before the model exceeded either a material temperature limit or a thermal stress limit. In order to reduce the thermal loading to the HDCR, the flowpath was coated with a 0.025” thermal barrier coating which reduced the incident heat flux to the model. The coating was composed of about 0.020” of zirconium dioxide and about 0.005” of Praxair Ni-171 which is a nickel base composite that served as a strain isolation layer. The thermal properties of the thermal barrier coating were provided by the engine manufacturer and verified through a literature survey (see Appendix A). The model included 10 fueling sites to permit testing of different injector stations and fueling schedules.

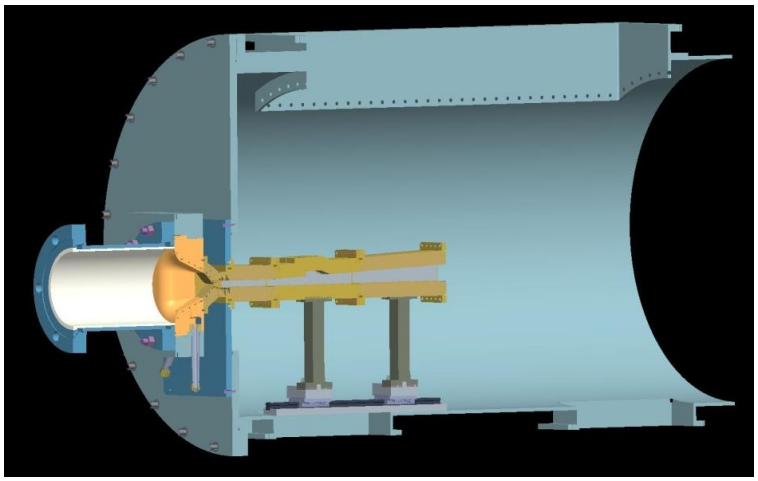

Figure 1. The HDCR in the AHSTF.

Simulated run conditions were dictated by the facility plenum total pressure and total enthalpy. For a typical run (see run 118.3 in Appendix B) simulating flight at Mach 5.84 and a flight dynamic pressure of 1030 lbf/ft^2 condition, the facility provided a total pressure of 213 psia and a total enthalpy of 721 Btu/lbm. The high pressure air was provided through a 5000 psia air system and the enthalpy was controlled by the arc-heater. Figure 2 illustrates a typical test sequence for a combustion test where relative thermal load is plotted against time. The events include: data recorders are started (1), the high pressure air supply is opened and the arc current is turned on (1-2), a tare is held at the test point (2-3), the fueling schedule is performed (4-5), a post fuel tare is performed (6-7), and the test concludes with a shutdown, venting, and purge of the facility (7-8).

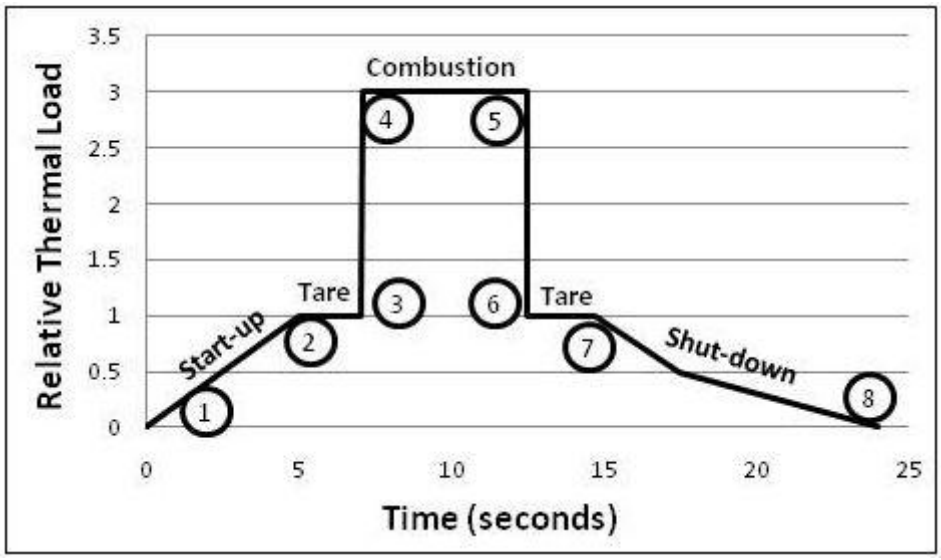

Figure 2. Sequence of events for a combustion run in the HDCR.

HDCR SENSOR SUITE AND LAYOUT

The heat flux transducers were provided by the Medtherm Corporation and were capable of measuring heating rates up to 500 Btu/ft^2-sec and maintained an accuracy of ±5%. Type-T thermocouples provided temperature measurements and were chosen for their compatibility with a copper wall. Thermocouple measurements with both uncoated and Zirconia coated beads and uncoated heat flux transducers were arranged so that a series of comparisons could be made during each run. A

three dimensional view of the HDCR model and a close-up of the instrumentation package as installed in the AHSTF is given in Figure 3. The model is instrumented with 144 pressure taps, 23 thermocouples, and 4 heat flux transducers along the flowpath. The pressure taps were placed along the centerline of the flowpath and across several span wise locations. Thirteen thermocouples and all heat flux transducers were offset by 0.75" from the centerline for either the cowl or the body side walls. Six thermocouples (3 for the port side and 3 for the starboard side) were placed along the sidewalls and 4 thermocouples were placed on the outer mold line (OML). A complete summary of the sensor arrangement is found Appendix C. To orient the reader (see Figure 4), the flowpath starts at axial station x=0.0" (which corresponds to the facility nozzle exit/isolator entrance), the base of the pilot cavity is at x=11.58", the beginning of the ramp/cavity closeout is at x=14.15", and the end of the ramp/cavity closeout is at x=15.79". Fueling can be provided at x=7.60", 9.60", 11.92", 16.5", and 19.75".

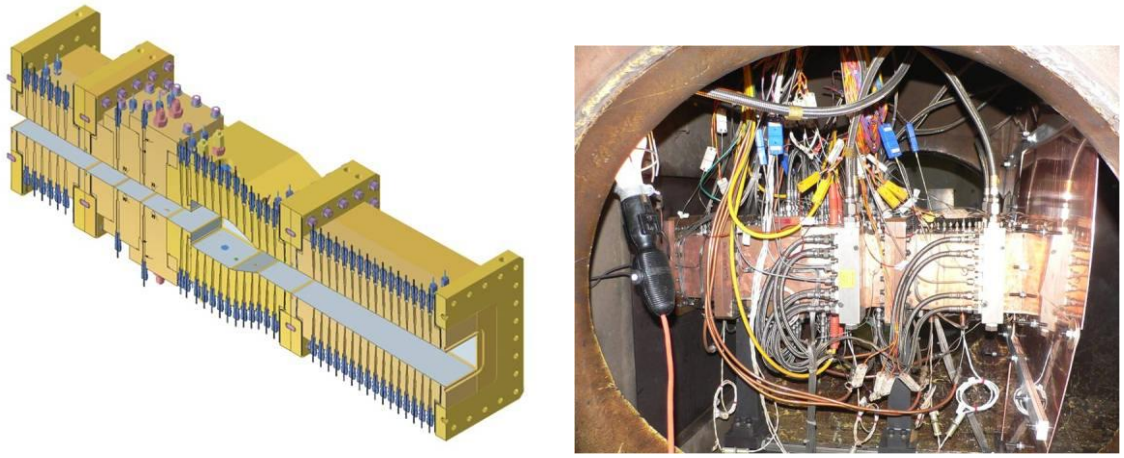

Figure 3. Three dimensional view of the HDCR instrumentation layout and a close-up view as installed in the AHSTF.

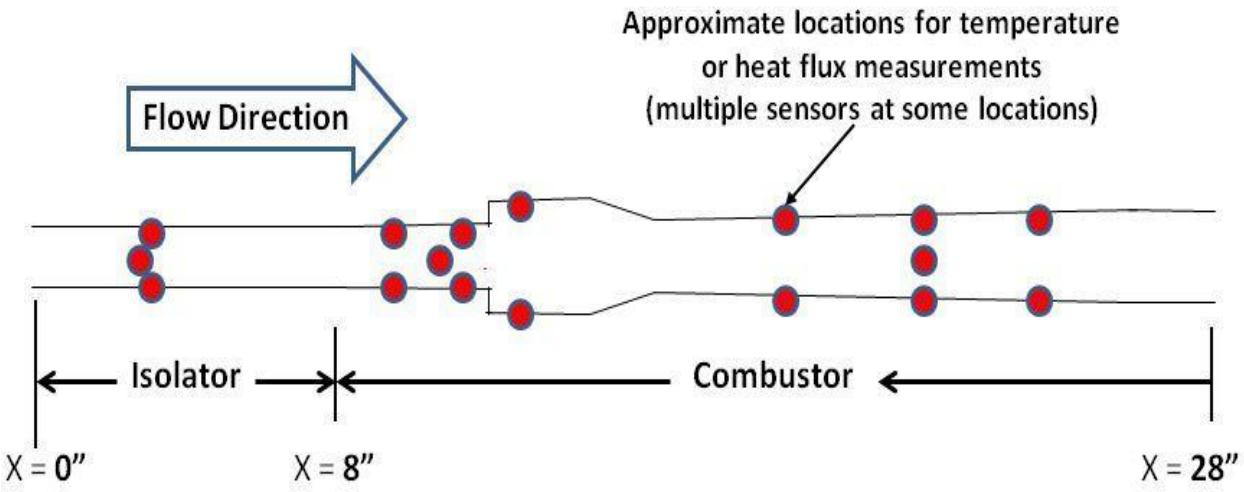

Figure 4. Approximate axial locations for HDCR temperature or heat flux sensors.

APPROACHES TO ESTIMATING HEAT FLUX

Heat flux and surface temperature measurements are needed for a variety of analytical efforts that support engine design and operability. Computational fluid dynamics simulations need wall conditions and thermal loading to complete the equations that provide a solution to the flow domain. Propulsion studies that estimate the thermal efficiency of an engine cycle can use these measurements to estimate heating losses to the ground test article. Since the engine model is protected with a thin thermal barrier coating, applying the same thermal barrier coating to the heat flux transducer would be the most direct way to get the desired measurement. Unfortunately, manufacturers of heat flux transducers warn against applying any kind of surface treatment to the sensing element as this would violate the calibration of the transducer and compromise the results. Thus, if heat flux transducers are going to be included in the instrument suite, they need to be unaltered and put in direct contact with the gas flow. Since the thermal environment of the ground tests is expected to be severe (heat fluxes on the order of 250-500 Btu/ft^2-sec), the use of a heat flux transducer will require a provision for water cooling of the transducer to avoid overheating the sensor. This further complicates any measurement as the water-cooled transducer and the surrounding wall will be at different temperatures.

An alternate approach for estimating heat flux without the use of a heat flux transducer involves a thermocouple measurement at the surface of the wall (references 7-9). This approach requires applying the temperature time history record to a conduction model of the wall to deduce the surface heat flux. This model has several limiting assumptions that must be satisfied to ensure that a proper evaluation can be made. A key assumption is that the material must be homogenous as the algorithm is based on the thermal properties of a single material. The application of the Zirconia coating would violate this type of approach as the thermal model would have a physical layup that was composed of two materials.

A third approach for determining surface conditions is to build a 1-D conduction model of the wall and use sub-surface temperature measurements to reconstruct the surface temperature. Models require an accurate depth measurement for the sensor and accurate material properties for each material layer. An initial guess of the surface temperature is made and the thermal model is run over the simulated time. The analytical result at the sub-surface location is then compared to the actual sensor measurement. Corrections to the surface boundary condition are made and the model is rerun. After a number of passes, the sub-surface prediction converges with the thermocouple measurement. This method works well for a single material and for some multilayer models. One major drawback that occurred in pursuing this approach for the present work is that attempts to establish a stable surface boundary condition were unsuccessful. This can happen for multilayer models where a highly conductive material is adjacent to a low conductivity insulator; thus, an alternate approach was selected.

THE INVERSE METHOD

The basic approach to estimating both the incident heat flux and wall temperature of the Zirconia coated surface begins with a description of the sensor layout used in the analysis (see Figure 5). The 2” copper wall (illustrated in green) is protected with a thin coating of Zirconia (illustrated in brown). The intermediate Praxair Ni-171 strain isolation layer was ignored for this analysis. The two sensors used in the analysis are the water-cooled heat flux transducer which penetrates the Zirconia surface and is flush with the flowpath and a thermocouple which is below the Zirconia surface and is located at the Zirconia/copper interface. When a thermal load is applied to the surface, the Zirconia wall will rapidly heat up, but the thermocouple readings below the surface will be significantly lower than if no thermal barrier were present. The heat flux transducer will also be exposed to the same thermal environment, but since it is water-cooled, the heating rate measured will be significantly higher than the Zirconia wall which is at an elevated temperature.

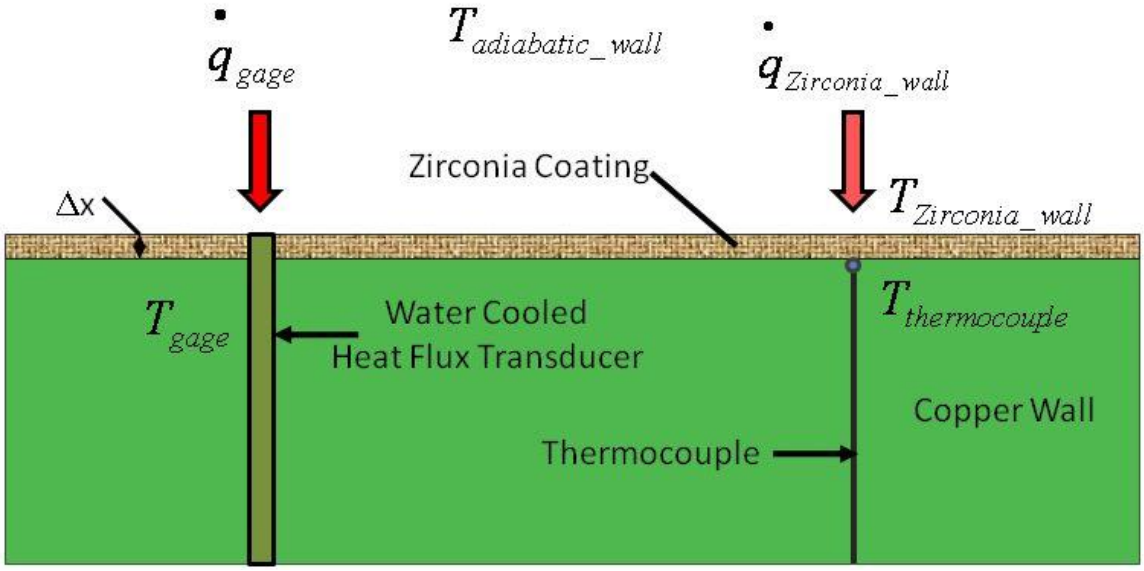

Figure 5. Schematic of the Zirconia coated copper wall.

A system of equations was developed to describe the heat flux to the wall. Starting with the definition of the Stanton Number, C_H, the heat flux to the wall, $\dot{q}_{Zirconia\_wall}$, can be expressed as:

$$\dot{q}_{Zirconia\_wall} = C_H \rho_{edge} u_{edge} (H_{adiabatic\_wall} - H_{Zirconia\_wall}) \quad \textbf{Equation 1}$$

where the driving potential for the aerodynamic heating to the surface is $H_{adiabatic\_wall} - H_{Zirconia\_wall}$, the enthalpy difference, and ρ_{edge} and u_{edge} are the density and flow velocity at the edge of the boundary layer, respectively (see reference 10, equation 6.85). The convective heat transfer coefficient, h, can be defined as:

$$h = C_H \rho_{edge} u_{edge} c_p \quad \textbf{Equation 2}$$

where the effective specific heat of the gas, c_p, is given by:

$$c_p = \frac{H_{adiabatic\_wall} - H_{Zirconia\_wall}}{T_{adiabatic\_wall} - T_{Zirconia\_wall}} \quad \textbf{Equation 3}$$

The heat flux that flows through the Zirconia wall, $\dot{q}_{Zirconia\_wall}$, can then be written as Equation 4, where it is equal to the product of the convective heat transfer coefficient, h_1, and the difference between the adiabatic wall temperature and the Zirconia wall temperature:

$$\dot{q}_{Zirconia\_wall} = h_1(T_{adiabatic\_wall} - T_{Zirconia\_wall}) \qquad \textbf{Equation 4}$$

By following the same steps as outlined above, the heat flux that is measured by the heat flux transducer, $\dot{q}_{gage}$, is equal to the product of the convective heat transfer coefficient, h_2, and the difference between the adiabatic wall temperature and the heat flux gage temperature (see Equation 5):

$$\dot{q}_{gage} = h_2(T_{adiabatic\_wall} - T_{gage}) \qquad \textbf{Equation 5}$$

Equation 6 describes the heat flux through the Zirconia layer. The heat flux is equal to the product of the Zirconia thermal conductivity, $k_{Zirconia}$, and the difference between the Zirconia wall temperature and the thermocouple temperature. This is further divided by the thickness, $\Delta x_{Zirconial}$, of the Zirconia layer:

$$\dot{q}_{Zirconia\_wall} = \frac{k_{Zirconia}}{\Delta x_{Zirconia}}(T_{Zirconia\_wall} - T_{thermocouple}) \qquad \textbf{Equation 6}$$

Equations 4, 5, and 6 contain ten variables that are needed to describe the heat flow through the model. Two variables, $\dot{q}_{gage}$ and $T_{thermocouple}$, are measured by the water-cooled heat flux transducer and the thermocouple, respectively. The material thermal conductivity, $k_{Zirconial}$, and the Zirconia coating thickness, $\Delta x_{Zirconial}$, are generally known quantities. This leaves three equations and six unknowns.

In order to establish a closed set of equations, several assumptions need to be made. The first assumption is that the convective heat transfer coefficients in equations 4 and 5 are equal:

$$h_1 \approx h_2 = h \qquad \textbf{Equation 7}$$

A second assumption is that, $T_{adiabatic\_wall}$, can be prescribed for the various flow and combustion conditions that will be tested. The adiabatic wall temperature can be determined from the recovery factor, r, which is defined by (see reference 10, equation 6.89):

$$r = \frac{T_{adiabatic\_wall} - T_{edge}}{T_{total} - T_{edge}} \qquad \textbf{Equation 8}$$

where T_{edge} is the temperature at the edge of the boundary layer and T_{total} is the total temperature of the gas which is prescribed for each test. Since T_{edge} is typically much smaller than either than $T_{adiabatic\_wall}$ or T_{total}, this equation can be approximated by:

$$T_{adiabatic\_wall} \approx rT_{total} \qquad \textbf{Equation 9}$$

For flows without combustion, the recovery factor for turbulent flow can be further related to the Prandtl number with equation 10 (reference 11):

$$r = \mathrm{Pr}^{1/3} \qquad \textbf{Equation 10}$$

A value of 0.72 was used which yielded a recovery factor of 0.896. The recovery factor for the combusting cases also utilized equation 10 with the Prandtl number being held fixed at 0.72. Reference 12 offered support for applying a constant value of Prandtl number for both the combusting and non-combusting cases. For flows where combustion is present, the total temperature is replaced with the adiabatic flame temperature of the combustion process to yield equation 11:

$$T_{adiabatic\_wall} = rT_{adiabatic\_flame} \qquad \textbf{Equation 11}$$

The flame temperature is determined by balancing the chemical equation of the products (generally air and fuel) and the resultant reactants of combustion. The enthalpy of the products is then balanced with the enthalpy of the reactants. The heat released in the combustion process raises the reactants to the flame temperature. This final temperature is dependent upon the fuel equivalence ratio and the initial temperature and pressure of the air.

With the adiabatic temperature defined as above, this reduces the solution set to three equations and four unknowns, T_{gage}, $T_{Zirconia\_wall}$, $\dot{q}_{Zirconia\_wall}$, and h. A final assumption which involves the heat flux transducer operating temperature can be made to close out the system of equations. Normally, a heat flux transducer would heat up at nearly the same rate as the wall in which it is installed. However, since the heat flux transducer selected for this study is water-cooled, the nominal operating temperature is expected to be no more than 350 °F. By making the assumption that the heat flux transducer heats up at the same rate as the surrounding wall until it reaches a prescribed temperature limit, the final set of equations is reduced to three equations and three unknowns. As will be shown later, the solution of the set of equations is relatively insensitive to the transducer temperature and this assumption does not impact the estimated heat transfer results.

At this point, the time history of heat flux transducer and thermocouple measurements of the ground test article can be applied to the governing equations. For each time step, the desired heat flux and wall temperature of the Zirconia wall can be deduced from the measurements. Having completed the system of equations and the solution methodology, this approach was applied to the combustion tests of the HDCR test article.

TEST CONDITIONS AND TESTING SERIES

Test conditions were established that were representative of the expected HIFiRE flight path. The test box for the program was bounded with Mach numbers between 5.5 to 8.5 and DP of 1000 to 3000 lbf/ft^2. The AHSTF has the capability to simulate the full range of Mach numbers to be evaluated. The range of DP that can be achieved is dictated by pressure limits of the facility. This limit decreases as enthalpy is increased. A DP of 3000 lbf/ft^2 can be achieved at the Mach 5.5 test condition and a DP of 1000 lbf/ft^2 can be achieved at the Mach 8.5 test condition (reference 13). The test gas in the AHSTF is dry air heated by an electric arc. To achieve the desired test points, three nozzles were constructed to simulate the flow entering the isolator at enthalpies corresponding to flight at Mach numbers 6, 7, and 8. The desired test points were generated by selecting one of the nozzles, tuning the injected total pressure, and varying the arc-heater to create the desired enthalpy. For the current work, data from the Mach 6 simulated tests were evaluated. Over 90 runs were made in this test series. Sensor data was taken at a 10 Hertz sampling rate. The model was fueled with ethylene for runs 107 to 121. A 64% ethylene and 36% methane mixture was used for runs 122 – 125.

RESULTS

Run 119.4 was selected to illustrate the results produced by the inverse method. As is shown in Figure 6, the test sequence as outlined in Figure 2 was followed and inflow parameters reached a near steady state condition after the t = 0.0 mark. Althought the total temperature, pressure and enthalpy did not vary appreciably during the test run, the fuel equivalence ratio, phi, varied in a prescribed manner.

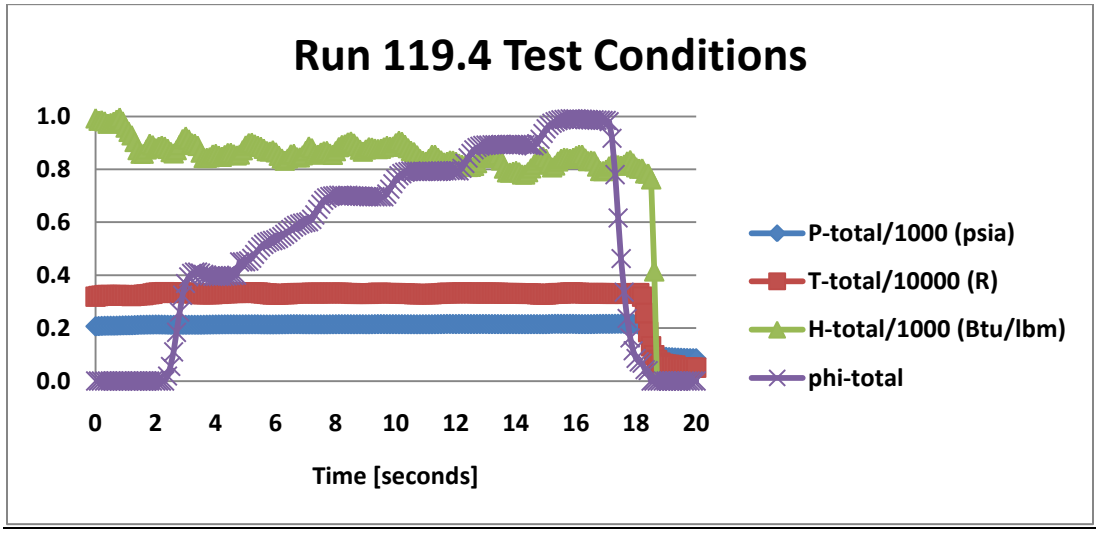

Figure 6. Test conditions for Run 119.4

The inverse method was applied to this run for the Zirconia coated thermocouple at axial station x=26". It was paired with the heat flux transducer at axial station x = 23" to complete the analysis. The method assumes that the two measurements are at the same location. Figure 7 shows that the heat flux transducer output reached 226 Btu/ft^2-sec. The inverse method was used to estimate the heat flux to the Zirconia wall for two cases, a ϕ = 1 and ϕ = 0.5 which were chosen to bracket the expected conditions in the flowpath. The estimated peak heat transfer to the Zirconia wall for the two cases was 147.7 and 140.7 Btu/ft^2-sec, respectively and translates to about a 35-38 percent reduction in heating to the wall when compared to the water-cooled heat flux transducer. Figure 8 shows that the Zirconia coated wall temperature for the ϕ = 1 and ϕ = 0.5 cases was 2159 and 2098 R, respectively.

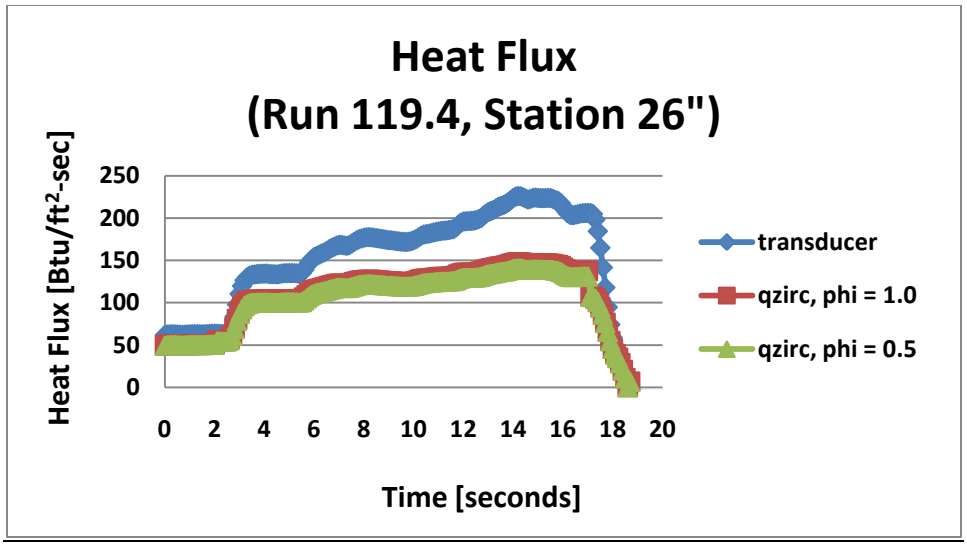

Figure 7. Heat flux at the Zirconia wall for Run 119.4 for ϕ = 1 and ϕ = 0.5.

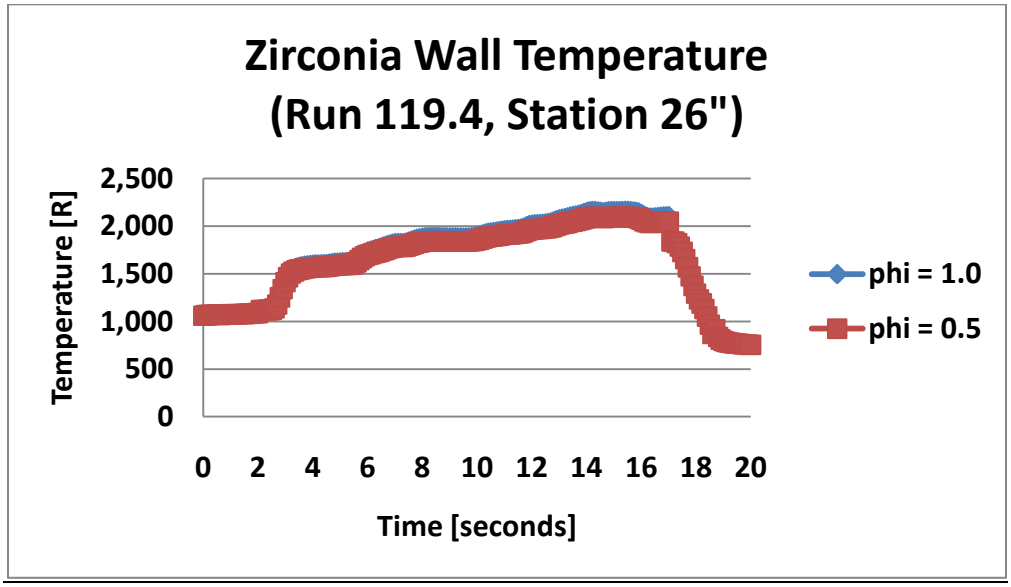

Figure 8. Zirconia wall temperature for Run 119.4 for ϕ = 1 and ϕ = 0.5.

Having established the process for estimating heat flux and wall temperature for a thermal barrier coated wall, the limiting assumption of assigning a maximum operating temperature for the water-cooled heat flux transducer could now be evaluated. For the Run 119.4, ϕ = 1 case, the sensitivity of the estimated Zirconia wall heat flux was evaluated for two limiting conditions of the transducer operating temperature. In case 1, the transducer operating temperature was allowed to heat up at the same rate as the copper wall. In case 2, the operating temperature was held to be a constant at the initial temperature of the copper wall, prior to the start of the run. Figure 9 shows that the resultant heat flux estimate is insensitive to the transducer operating temperature.

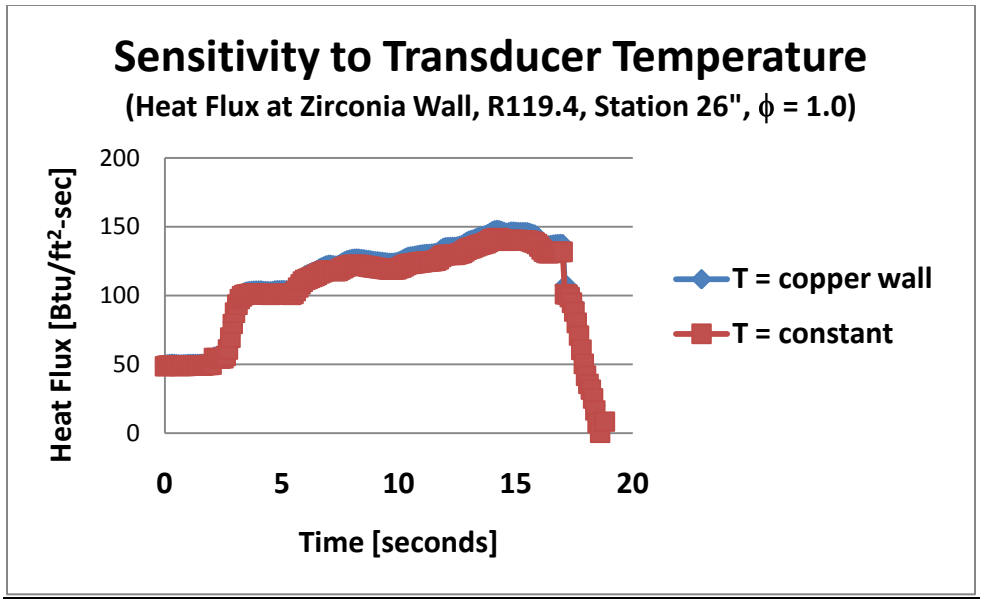

Figure 9. Inverse method sensitivity to heat flux transducer operating temperature.

CONCLUSIONS

The HIFiRE HDCR provided numerous combustion tests of an engine flowpath at hypersonic conditions using both ethylene and an ethylene/methane fuel mixture. In attempting to estimate the heat flux and wall temperature of the Zirconia coating along the flowpath of the HDCR, it was found that traditional methods were not useful in providing the desired result. Heat flux transducer suppliers recommended that sensors be free of any surface treatment (Zirconia coating) as this would impact the calibration of the instrument. Surface thermocouples which are often used to deduce a heat flux measurement could not be used directly as the Zirconia coating would violate a limiting assumption that the wall must be homogeneous. In addition, deducing a heat flux measurement with just a sub-surface temperature measurement was problematic as the method required the establishment of a stable surface temperature boundary condition. The thermal conductivity mismatch between the Zirconia and copper materials prevented this approach from succeeding.

In order to deduce the required measurements with the instrument suite available in the HDCR ground tests, an inverse method was developed which utilized an uncoated water-cooled heat flux transducer and a Zirconia coated thermocouple. A set of equations was developed which governed the heat flow into the HDCR wall. This algorithm was applied to several test runs of the HDCR to obtain the surface conditions of the Zirconia coating. Estimates were made for two fuel equivalence ratios ($\phi = 1.0$ and 0.5) and showed that the heat flux varied by about 4 % and the Zirconia wall temperature varied by less than 3 %. The variance in the heat flux transducer operating temperature was also shown to have only a small effect upon the estimated heat flux at the Zirconia wall. This analytical approach provides a capability for estimating the surface conditions of the Zirconia wall with two measurements: a heat flux transducer flush with the flowpath and a sub-surface temperature measurement located below the Zirconia coating on the surface of the copper wall. These results can support engine designers who require flowpath boundary conditions for computational fluid dynamics simulations and in estimating the heat balance of the engine cycle.

ACKNOWLEDGEMENTS

The authors wish to thank Diego Capriotti and Ed Ruf for their support in the design of the thermal characterization instrumentation and in the interpretation of the results for the HIFiRE Direct Connect Rig. We also want to thank Robert Baurle and Ken Rock who provided support in the development of the equations used in this analysis.

ACRONYMS

AFRL	U.S. Air Force Research Laboratory
AHSTF	Arc-Heated Scramjet Test Facility
DSTO	Australian Defence Science and Technology Organization
HDCR	HIFiRE Direct Connect Rig
HIFiRE	Hypersonic International Flight Research Experimentation
OFHC	Oxygen Free High Conductivity
OML	outer mold line

SYMBOLS

C_H	Stanton Number (non-dimensional)
c_p	specific heat (Btu/lbm-R)
DP	dynamic pressure (lbf/ft^2)
H	enthalpy (Btu/lbm)
h	convective heat transfer coefficient (Btu/ft^2-sec-R)
k	thermal conductivity (Btu/sec-ft-R)
p	absolute pressure (lbf/in^2)
Pr	Prandtl number (non-dimensional)
$\dot{q}$	heat flux (Btu/ft^2-sec)
r	recovery factor (non-dimensional)
T	temperature (R)
t	time (seconds)
u	velocity (ft/sec)
x	axial station (inches)
Δx	Zirconia coating thickness (inches)
ρ	density (lbm/ft^3)
ϕ or phi	fuel equivalence ratio (non-dimensional)

REFERENCES

1. Guy, R. W., Rogers, R. C., Puster, R. L., Rock, K. E., and Diskin, G. S., "The NASA Langley Scramjet Test Complex," AIAA-96-3243, 1996.

2. McClinton, C., "X-43: Scramjet Power Breaks the Hypersonic Barrier," Dryden Lecture Series, 44th AIAA Aerospace Sciences Meeting and Exhibit, Reno, Nevada, January 9, 2006.

3. Jackson, K. R., Gruber, M. R., Jackson, T. A. and Hass, N. E., "HIFiRE Flight 2 Scramjet Flight Experiment Overview," 55th JANNAF Propulsion Meeting, Boston, Massachusetts, May 12-16, 2008.

4. Thomas, S. R. and Guy, R. W., "Expanded Operational Capabilities of the Langley Mach 7 Scramjet Test Facility," NASA Technical Paper 2186, 1983.

5. Thomas, S. R. and Guy, R. W., “Increased Capabilities of the Langley Mach 7 Scramjet Test Facility,” AIAA/SAE/ASME 18th Joint Propulsion Conference, June 21-23, 1982, Cleveland, Ohio, AIAA-82-1240.

6. Custodio, T., Riberio, G., and Morales, S., “Direct Connect for Hypersonic International Flight Research Experimentation (HIFiRE) Critical Design Review,” August 27, 2007.

7. Cook, W. J., “Determination of Heat-Transfer Rates from Transient Surface Temperature Measurements,” AIAA Journal, Volume 8, No. 7, pp. 1366-1368, July 1970.

8. Schultz, D. L. and Jones, T. V., “Heat-Transfer Measurements in Short-Duration Hypersonic Facilities,” AGARD-AG-165, February 1973.

9. Hollis, B. R., “User’s Manual for the One-Dimensional Hypersonic Aero-Thermodynamic (1DHEAT) Data Reduction Code,” NASA Contractor Report 4691, August 1995.

10. Anderson, J. D., Jr., Hypersonic and High Temperature Gas Dynamics, McGraw-Hill, Inc., 1989, pp. 248-249.

11. Bertin, J. J., Hypersonic Aerothermodynamics, AIAA Education Series, Inc., Third Printing, 1994, p. 340.

12. Poferl, D., J., Svehla, R. A., and Lewandowski, K., “Thermodynamic and Transport Properties of Air and the Combustion Products of Natural Gas and of ASTM-A-1 Fuel with Air,” NASA TN D-5452, October 1969.

13. Hass, N. E., Cabell, K. F., and Storch, A. M., “HIFiRE Direct-Connect Rig (HDCR) Ground Test Results from the NASA Langley Arc-Heated Scramjet Facility, presented at the 43rd CS/31st APS/25th PSHS JANNAF meeting, La Jolla, California, December 7-11, 2009.

14. Wang, Z., “Thermophysical and Mechanical Properties for Glid-Cop,” Argonne National Laboratory, January 4, 1991.

15. Durrani, S. K., Akhtar, J., Ahmad, M., and Hussain, M. A., “Synthesis and characterization of low density calcia stabilized Zirconia ceramic for high temperature furnace application,” Materials Chemistry and Physics, Volume 100, pp. 324-328, 2006.

16. Victor, A. C., and Douglas, T. B., “Physical Properties of High Temperature Materials,” National Bureau of Standards, WADC Technical Report 57-374, Part VI, December 1960.

17. McPherson, R., “A Model for the Thermal Conductivity of Plasma-Sprayed Ceramic Coatings,” Thin Solid Films, Volume 112, 1984, pp. 89-95.

18. Chen, Z., Speakman, S., Howe, J., Wang, H., Porter, W., and Trice, R., “Investigation of reactions between vanadium oxide and plasma-sprayed yttria-stabilized Zirconia coatings,” Journal of the European Ceramic Society, Vol. 29, pp. 1403-1411, 2009.

19. Cao, X. Q., Vassen, R., and Stoever, D., “Ceramic materials for thermal barrier coatings,” Journal of the European Ceramic Society, Volume 24, pp. 1-10, 2004.

APPENDIX A – SELECTED MATERIAL PROPERTIES

Material	Density [lbm/ft^3]	Specific Heat [Btu/lbm-F]	Thermal Conductivity [Btu/hr-ft-F]	Melting Point [F]
OFHC copper (reference 14)	558	0.092	203.0	1981
plasma sprayed zirconium dioxide	207 (reference 15)	0.20 (reference 16)	0.63 (refs 17 & 18)	4890 (reference 19)

APPENDIX B – TEST CONDITIONS FOR SELECTED RUNS

Run #	Flight Mach #	T_{total} (R)	P_{total} (psia)	H_{total} (Btu/lbm)	ϕ	$T_{adiabatic\_flame}$ (R)
118.3	5.84	2754	213	721	1.0	5069
					0.5	4401
119.4	6.5	3306	214	884	1.0	5240
					0.5	4705
123.3	6.5	3327	214	891	1.0	5207
					0.5	4680

APPENDIX C – THERMAL INSTRUMENTATION SUMMARY

Axial Station (inches)	Heat Flux Transducers	Zirconia Coated Thermocouples	Bare Thermocouples	Zirconia Coated Port Sidewall Thermocouples	Zirconia Coated Starboard Sidewall Thermocouples	Outer Mold Line Bare Thermocouples
2.38				T2P0238I	T2S0238I	
3.00	H3C0030OO	T2B0300OO				T2O0300OO
11.00		T3B1100OO	T3C1100OO			
12.75				T3P1275I	T3S1275I	
13.75	H4C0138OO	T3B1375O T3B1375OO	T3C1375O			T3O1375OO
14.50		T3B1450OO T3B1450O	T3C1450O			
20.50	H4C0205OO	T4B2050OO				T4O2050OO
23.00	H4C0230OO		T4B2300OO	T4P2300I	T4S2300I	T4O2300OO
26.00		T4B2600OO	T4C2600OO			